

Sticky elastic collisions

JÉRÉMIE BEC¹, STEFANO MUSACCHIO²,
AND SAMRIDDHI SANKAR RAY^{1,3}

¹ Laboratoire J.L. Lagrange UMR 7293, Université de Nice Sophia Antipolis, CNRS,
Observatoire de la Côte d’Azur, BP4229, 06304 Nice Cedex 4, France.

² Laboratoire J.A. Dieudonné UMR 7351, Université de Nice Sophia Antipolis, CNRS, Parc
Valrose, 06108 Nice, France.

³ International Centre for Theoretical Sciences, Tata Institute of Fundamental Research,
Bangalore 560012, India.

(Received 21 December 2012)

The effects of purely elastic collisions on the dynamics of heavy inertial particles is investigated in a three-dimensional random incompressible flow. It is shown that the statistical properties of inter-particle separations and relative velocities are strongly influenced by the occurrence of *sticky elastic collisions* — particle pairs undergo a large number of collisions against each other during a small time interval over which, hence, they remain close to each other. A theoretical framework is provided for describing and quantifying this phenomenon and it is substantiated by numerical simulations. Furthermore, the impact of hydrodynamic interactions is discussed for such a system of colliding particles.

1. Introduction

Dust, droplets, bubbles, and other finite-size particles suspended in turbulent flows are common in nature (see, e.g., Csanady 1980; Post & Abraham 2002; Shaw 2003). Their statistical properties are very different from that of tracers, i.e. point-like particles with the same mass density as the advecting fluid. Indeed, when the suspended particles have a finite size and a density different from that of the fluid, inertial effects become important. Consequently, the motion of particles starts differing from the underlying flow. This results in intricate correlations between the particle positions and the geometry of the turbulent flow. Heavier particles are expelled from vortical structures while lighter particles concentrate in their cores. A consequence of these mechanisms is the presence of strong fluctuations in the spatial distribution of particles. This phenomenon, known as *preferential concentration*, has been the subject of extensive research in fluid dynamics for the last decades (see Douady *et al.* 1991; Squires & Eaton 1991).

Another consequence of inertia is that particles are likely to be very close to each other with large velocity differences. The process leading to such events, known either as the sling effect (Falkovich *et al.* 2002) or the formation of caustics (Wilkinson & Mehlig 2005), has been extensively measured and studied during the past ten years (see, e.g., Bec *et al.* 2010; Salazar & Collins 2012). The presence of such spatial inhomogeneities is known to strongly alter possible interactions between particles. Since the pioneering work of Saffman & Turner (1956) motivated by coalescences of cloud droplets, much work has been devoted to understanding the rate at which heavy inertial particles collide. A commonly adopted approach consists in assuming that the inter-collision time is much longer than the convergence timescale of particle dynamics to a statistically stationary regime. This premise, which is asymptotically true in the limit of very dilute suspensions, entitles counting collisions without having to effectively perform them. The frequency at

which such *ghost particles* collide is then a time-independent statistical observables that can be quantified as a function of particle sizes and response times. Several studies have assumed this ghost-particle hypothesis in order to estimate collision rates of heavy inertial particles in turbulent flows (see, e.g., Sundaram & Collins 1997; Falkovich *et al.* 2002). However, little is known about the limits of such an approach. For instance, an important statistical weight is given to events when two concentrated clouds of particles cross each other with a large velocity difference. It is clear that the very-dilute approximation should then fail and that multiple-collisions are likely to occur. We report in this paper results on the effects of actual collisions on the dynamics and statistics of inertial particles transported by a non-stationary fluid flow.

The simplest framework for treating short-range collective effects in the particle dynamics is to consider an ensemble of hard spheres that are suspended in a prescribed flow and which undergo purely elastic (momentum and energy preserving) collisions with each other. Such a system, in the absence of any underlying fluid transport, has long been a paradigmatic model in statistical mechanics. It is the basis of the kinetic theory of gasses, in which it is assumed that the kinetic energy is conserved both by the collisions and by the dynamics of each particle. If we allow for a certain amount of inelasticity in the collisions a suitable model for granular gasses is obtained (see Goldhirsch 2003, for a review). A peculiar behaviour of such granular systems is the spontaneous aggregation of particles. Since inelasticity implies the loss of a finite percentage of kinetic energy at each collision, the particles can eventually stick together leading to the formation of large clusters. However, this effect occurs also in settings that are not common in studies of granular media. Indeed, as we will see in this work, it suffices that kinetic energy dissipation occurs not via collisions but rather through individual particle dynamics. This is the case for heavy inertial particles whose motion is dominated by viscous damping and which undergo purely elastic collisions. We show that the clustering phenomenon emerging in such systems originates from what we call *sticky elastic collisions*. During these events, the particles bounce many times against each other and energy is dissipated during their motion between successive collisions. This mechanism has strong influences on the statistics of inter-particle distances and relative velocities. Furthermore, to validate the presence of this effect in real settings, we study the influence of hydrodynamic interactions and show that they cannot prevent sticky elastic collisions from occurring.

This paper is organised as follows. In §2, we discuss the equations of motion of the inertial particles and recall some key results, in the absence of any collisions, on preferential concentration. In §3, we present numerical results and provide an asymptotic analysis for the phenomenon of sticky elastic collisions in the absence of hydrodynamic interactions. We then discuss the effect of hydrodynamic interactions in §4 by considering far-field interactions. We make some concluding remarks and summarise our results, as well as provide a perspective for future work, in §5.

2. The Model

To set the stage, we begin by recalling the basic physics of a system of N small hard spheres which are in a random, time-dependent, incompressible fluid field $\mathbf{u}(\mathbf{x}, t)$ and are subject to viscous dissipation. When such particles have a small Reynolds number and are much heavier than the fluid, they interact with the flow by Stokes viscous drag and their trajectories $\mathbf{x}_i(t)$ are determined by Newton's law:

$$\dot{\mathbf{x}}_i = \mathbf{v}_i, \quad \dot{\mathbf{v}}_i = -\frac{1}{\tau} [\mathbf{v}_i - \mathbf{u}(\mathbf{x}_i, t)] \quad i \in [1, N] \quad (2.1)$$

where τ is the viscous-drag relaxation (Stokes) time defined via $\tau = 2\rho_p a^2 / (9\rho_f \nu)$, where ρ_p is the particle density, ρ_f the fluid density, ν its kinematic viscosity, and a is the particle radius. The Stokes number is a measure of the inertia of the particle and is defined as $St = \tau/\tau_f$, where τ_f is a characteristic timescale of the fluid flow. In this work, we additionally introduce interactions between particles in the following sense. The particles interact through elastic collisions which, for the case of spherical particles of equal size and mass, correspond to an exchange of the radial component of the velocities of the two colliding particles upon impact, namely when $|\mathbf{x}_i - \mathbf{x}_j| = 2a$.

The clustering phenomenon occurs naturally, independently of the carrier flow compressibility, for an ensemble of particles which evolve according to Eq. (2.1), even in the absence of interactions or collisions between particles. We note that the case of no collisions is equivalent to the ghost particle approach. The physical mechanisms which lead to strong inhomogeneities in the spatial distribution of particles arise from the underlying dissipative chaotic dynamics: The system is characterised by a constant contraction rate d/τ in the position-velocity phase space which drives the particles towards a dynamically evolving fractal set. The clusters of particles are the projection of such fractals on the position space. The fractal dimensions of particles distribution provide a convenient tool to quantify their clustering (see Bec *et al.* 2007; Calzavarini *et al.* 2008). In particular the correlation dimension D_2 is defined via the power-law behaviour of the probability distribution function (PDF) of inter-particle distances $p_2(r) \sim r^{D_2-1}$ (see the inset of Fig. 1a for particles with different Stokes numbers in a three-dimensional random flow). Note that the density $p_2(r)$ is such that the probability that two particles are at a distance between r and $r+dr$ is $p_2(r) dr$ and relates to the radial distribution function $g(r)$: in three dimensions, one has $g(r) = 4\pi r^2 p_2(r)$.

The intensity of clustering is influenced by the properties of the velocity field $\mathbf{u}(\mathbf{x}, t)$ and in particular by its spatial and temporal correlations. Here we will assume that the velocity is differentiable in space and time and characterised by unique time and length scales. Let us denote by L_f the fluid flow correlation length, which is assumed much larger than the particle radius a , and by τ_f its correlation time, which is of the same order as the turnover time L_f/U where U is the typical amplitude of \mathbf{u} . In the limit of vanishing dissipation $St = \tau/\tau_f \rightarrow 0$, Eq. (2.1) becomes that of tracers, namely $\dot{\mathbf{x}}_i = \mathbf{u}(\mathbf{x}_i, t)$, and the incompressibility condition $\nabla \cdot \mathbf{u} = 0$ ensures a uniform distribution of particles. Particles distribute uniformly also in the opposite limit $St \rightarrow \infty$, in which the force acting on particles become very small so that they follow almost a ballistic motion and fill the whole position-velocity phase-space. The maximum of clustering is achieved for intermediate (order-unity) values of St where the minimum of the fractal dimension is reached.

Clearly, the presence of collisions will affect the particle distribution on scales of the order of their size. Heuristically, one expects the two-particle distribution $p_2(r)$ to be unchanged at separations r much larger than the interaction distance $2a$. At separations of the order of $2a$, the elastic collisions decorrelate the particle dynamics from the carrier flow. Naively, one would then expect that the particles distribute like an ideal gas at such scales, and consequently have a uniform distribution. In dilute systems, the crossover between these two regimes would occur at a scale given by the distance travelled by the particles before it relaxes to its attractor. This distance can be written as $r_\star = \tau v_c(St)$, where v_c is the typical velocity difference at collisions. However, as seen from the inset of Fig. 1a, this naive picture seems wrong. As we will see in the next section, we indeed find that the two-particle density p_2 diverges when $r \rightarrow 2a$. This effect is due to the presence of sticky elastic collisions.

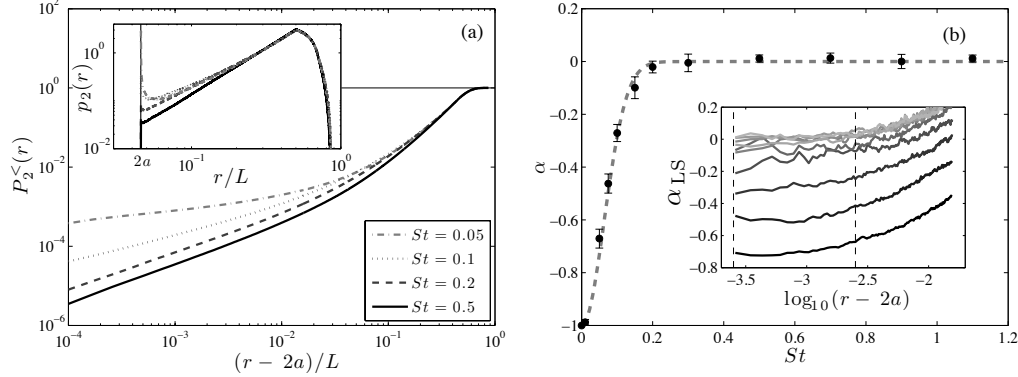


FIGURE 1. (a) Log-log plot of the cumulative probability distribution $P_2^<(r)$ as a function of $(r-2a)$ for some representative values of St as indicated in the legend. Inset: Log-log plot of the two-particle density $p_2(r) = dP_2^<(r)/dr$ as a function of r for the same values of St . (b) Exponent α versus St . The gray dashed line is an empirical fit of the form $-\exp(-(St/0.09)^2)$. Inset: local slopes $\alpha_{LS} = d \log P_2^<(r-2a)/d \log(r-2a) - 1$ as a function of $(r-2a)$ for various St . The two dashed vertical lines indicate the region over which we calculate the mean and the standard deviation of α_{LS} .

3. Particle adhesion through recurrent collisions

To investigate the effect of collisions on clustering we resort to numerical simulations of Eq. (2.1). For simplicity and without any loss of generality, we consider two ($N = 2$) particles in a three-dimensional cubic domain of size L with periodic boundary conditions. The velocity field is obtained from a superposition of Fourier modes whose amplitudes are stochastic Ornstein-Uhlenbeck processes with Gaussian statistics and a correlation time τ_f . The amplitude of each mode, which has a standard deviation of the order of L/τ_f , is chosen to ensure statistical isotropy at small scales. In our simulations we use several values of τ with Stokes numbers $St = \tau/\tau_f$ lying between 0.01 and 1.1. We have done simulations with various values of the particle radius a , but report here results obtained for $a \approx 0.02$. Our time marching is an implicit Euler scheme with a fixed time step $\delta t = 10^{-4}$ when the particles are far away from each other. However, when the particles are close to each other, the time step is adapted in order to resolve collisions with a high accuracy.

Our numerical simulations reveal a very interesting, hitherto unknown, phenomenon which is clearly absent in the collisionless or ghost-collision case. As expected the effects of collisions on the spatial distribution of particles, as characterised by the PDF of inter-particle distance, are negligible for particle separations much larger than $2a$. However collisions dramatically affect the statistics of pair-separations at small scales. In particular, the probability distribution function of the inter-particle distance $p_2(r)$ displays a power law behaviour $p_2(r) \sim (r-2a)^\alpha$ for distances close to the cutoff $2a$. The exponent α is a monotonically increasing function in the Stokes number St : It begins with the value -1 for $St \rightarrow 0$ and approaches 0 as $St \rightarrow \infty$. Figure 1a shows the cumulative probability distribution $P_2^<(r)$, which is the probability of finding two particles at a distance less than r , as a function of $(r-2a)$, on a log-log scale, for some representative values of St that we use in our simulations. We clearly find that $P_2^<$ behaves as a power law $\propto (r-2a)^{\alpha+1}$ at small values of $r-2a$. From a local slope analysis we extract the local scaling exponent $\alpha_{LS} = d \log P_2^<(r-2a)/d \log(r-2a) - 1$ (see the inset of Fig. 1b); the mean of this gives us a measure of the scaling exponent α and the standard deviation an estimate of the error. In Fig. 1b we show the behaviour of α as a function

of the Stokes number. The gray dashed line is a fit to our numerical data and is given by $-\exp(-(St/0.09)^2)$. In the inset the dashed vertical lines denote the region over which we calculate the mean and the standard deviation to obtain α . Two asymptotic values are clearly visible on Fig. 1b: one observes that $\alpha \rightarrow 0$ when $St \rightarrow \infty$ and $\alpha \rightarrow -1$ when $St \rightarrow 0$. Note that the stiffness of the system in the limit $St \rightarrow 0$ prevents us from obtaining accurate numerical results in this limit. Nevertheless, our data show a monotonic convergence towards $\alpha = -1$. These two asymptotic values of the exponent are signatures of two different collision mechanisms.

For large Stokes numbers the motion of particles is weakly correlated with the local values of the fluid velocity field, because it is determined by the cumulative contributions of the flow integrated over the particle trajectories with a long memory kernel. Close to the collision distance individual particle velocities are almost uncorrelated and vary on very large timescales. The relative motion of the two particles is therefore almost ballistic, with a random relative velocity. The time that the two particles spend at a distance between r and $r + dr$ is given by $dt = V dr$, where V is a their typical velocity difference. This leads to $p_2(r) \sim (r - 2a)^0$ thus yielding $\alpha \rightarrow 0$ when $St \rightarrow \infty$.

The limit $St \rightarrow 0$ is more complicated. In this case the motion of the particles is strongly correlated with the fluid velocity field \mathbf{u} , and therefore particles typically arrive at colliding distances with a very small relative velocity, of the order of the fluid velocity difference, namely $2a\sigma$, where σ is the local gradient of \mathbf{u} . After the collision they tend to separate but the fluid velocity field quickly brings them back together, because of the short relaxation time $\tau \ll \tau_f$. Particles then collide again and this mechanism will, therefore, lead to a long series of high-frequency collisions during which the particle remain within a distance of the order of $2a$. Next, to quantify the effects of these events on the statistics of inter-particle distance, let us consider a simple, one dimensional model for the separation $r = |\mathbf{x}_1 - \mathbf{x}_2|$ and the radial relative velocity $v = (\mathbf{v}_1 - \mathbf{v}_2) \cdot \hat{\mathbf{r}}$ of two particles, between two collisions occurring at time t_n and t_{n+1} . The equations of motion can be written as

$$\dot{r} = v, \quad \tau \dot{v} = -v - 2a\sigma. \quad (3.1)$$

Here, we have assumed that the fluid velocity gradient $-\sigma < 0$ remains constant. This is justified because particle dynamics is much faster than the correlation time of the fluid velocity ($\tau \ll \tau_f$). Also, we have neglected higher-order terms in the Taylor expansion of \mathbf{u} . The above equation gives $r(t) = 2a - \tau(v_n + 2a\sigma)[\exp(-t/\tau) - 1] - 2a\sigma t$ and $v(t) = v_n \exp(-t/\tau) + 2a\sigma[\exp(-t/\tau) - 1]$ where v_n is the relative radial velocity immediately after the n -th impact at time t_n . Introducing the small parameter $\epsilon_n = v_n/(2a\sigma)$ and Taylor expanding the above expressions for $t/\tau \ll 1$ one obtains a recursive relation for the relative velocity at collision, namely $\epsilon_{n+1} = \epsilon_n(1 - 2\epsilon_n/3)$, which leads to $v_n \sim 2a\sigma/n$. The inter-collision time $\theta_n = t_{n+1} - t_n$ decreases as $\theta_n \sim \tau/n$, and the maximum distance r^* reached by the two particles in the excursion between two collisions scales as $\delta = r_n^*/(2a) - 1 \sim \sigma\tau/n^2$. The number of collisions increases exponentially in time $n_c \sim \exp(Ct/\tau)$, with $C > 0$, and the inter-particles distance goes to 0. We call this phenomenon *sticky elastic collisions*. Note that the series defined by the sum of inter-collision times $\sum_n \theta_n$ is not converging. This ensures that the number of collisions does not become infinite in a finite time, at variance with the case for inelastic collisions where the particles eventually collapse and aggregate. In the case of the one-dimensional sticky elastic collisions, the recurrent process stops only when the fluid velocity gradient becomes positive (for $t \simeq \tau_f$) and takes the two particles far away. During any one of these events, only the first m collisions will contribute to the probability of having the two particles at a distance larger than $r \simeq 2a(1 + \sigma\tau/m^2)$. The fraction of time spent at a

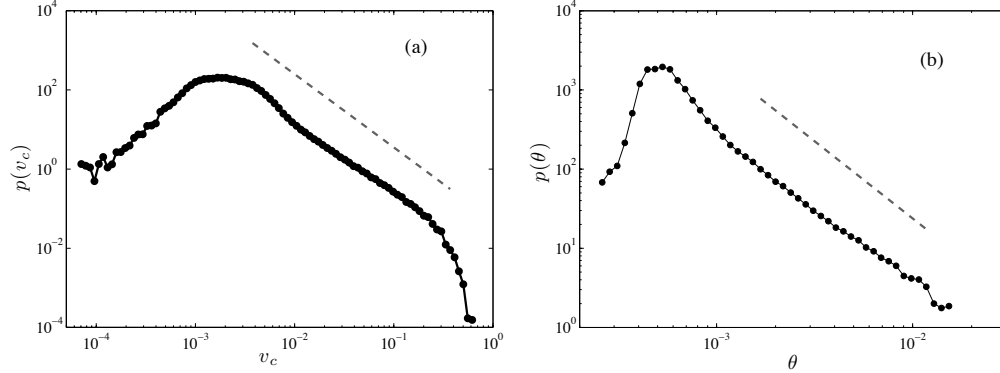


FIGURE 2. (a) Log-log plot of the PDF of inter-collision radial velocity v_c for $St = 0.01$; the dashed line shows a scaling of -1.85 . (b) Log-log plot of the PDF of inter-collision time θ for $St = 0.01$; the dashed line shows a scaling of -1.95 .

distance larger than r is thus $\sim \sum_{n < m} \theta_n \sim \ln m \sim -\ln(r - 2a)$. This gives for the PDF of inter-particle distances $p_2(r) \sim (r - 2a)^{-1}$, yielding the asymptotic value $\alpha \rightarrow -1$ for $St \rightarrow 0$.

The heuristic arguments developed here to quantify the statistical signature of sticky events are purely one-dimensional. However, they extend to higher dimensions by geometrical considerations. The one-dimensional case would hold true if the velocity difference \mathbf{v} between the particles were exactly aligned with their separation \mathbf{r} . A misalignment leads to rebounds of the two particles at different locations on their surfaces. For spherical particles, this implies that better is the alignment between \mathbf{v} and \mathbf{r} , higher is the number of successive secondary collisions. Statistically, this implies that the distribution of distances is dominated by almost head-on collisions, which can essentially be treated as a one-dimensional problem. The space dimensionality should just appear as a multiplicative factor in the power-law behaviour at $r \rightarrow 2a$.

The effects of these events are detectable also in the statistics of inter-collision times θ and relative radial velocity at collision v_c . Within the model derived above, for $St \rightarrow 0$, we obtain $p(v_c) \sim v_c^{-2}$ and $p(\theta) \sim \theta^{-2}$. In Fig.(2a) and Fig.(2b) we show a log-log plots of $p(v_c)$ versus v_c and $p(\theta)$ versus θ , respectively, obtained from simulations for $St = 0.01$; the dashed lines show a scaling exponent of ≈ -1.9 in each case. We have checked the scaling becomes significantly shallower and the extent of scaling gets progressively reduced with St increases. Note that a similarly steep increase of the inter-collision time distribution at small values has been observed by Ten Cate *et al.* (2004) in full direct numerical simulations of finite-size particles suspended in a viscous flow. This effect has been interpreted as a possible consequence of lubrication forces between the particles that makes the particles remain close to each other for long times. In the next section, we will comment on the influence of hydrodynamical interactions on sticky elastic collisions. Nevertheless it is worth stressing here that lubrication is not necessary to obtain multiple collisions between particles.

The tails of $p(v_c)$ and $p(\theta)$ at small values seem to indicate that they cannot be normalised. However, we observe for small but finite values of St , a cutoff at the smallest values of v_c and θ , which prevents this divergence. Indeed, the power-law behaviours are due to typical sticky events. As we have seen, the number of collisions is of the order of $n_c \sim \exp(C/St)$. Therefore, the minimal collisional velocity and inter-collision time are both $\propto 1/n_c \sim \exp(-C/St)$. The power-law is thus just appearing in intermediate ranges, namely $(2a/\tau_f) \exp(-C/St) \ll v_c \ll (2a/\tau_f)$ and $\tau \exp(-C/St) \ll \theta \ll \tau$. The

events leading to values smaller than the lower bounds are related to situations where the fluid velocity gradient is maintained negative for an exceptionally long time. This happens with an inverse-Gaussian probability in a finite-correlation-time flow, whence the cutoff. Also, the extension of this argument to the singular limit $St = 0$ is far from obvious. Note finally that in dimensions higher than one, the geometrical considerations explained above should also provide a cut-off for very small collision times and velocities.

4. Effect of hydrodynamic interactions

In this section, we address the question whether or not sticky elastic collisions can be observed in realistic flows. For that, it is important to know how far the observations and conclusions drawn above are valid when we, in addition to collisions, introduce hydrodynamic interactions between particles. To answer this question, we take into account the far-field or long-range interactions and assume that it is valid all the way to the smallest separations. This approach yields several interesting results which we discuss below. Of course this assumption, in reality, breaks down when particles approach *very* close to one other. However in that case, either lubrication leads to an effective increase in the particle physical radius or, in the case when the velocity difference is too large, hydrodynamics might not be a valid description of the interactions between the particles.

In its simplest formulation, the long-range hydrodynamic interactions between particles in a flow is taken into account by considering the perturbation in the ambient fluid velocity field, as experienced by an individual particle, because of the motion of all the other particles. Thus the effective velocity field acting on any particle is a superposition of the unperturbed (turbulent) advecting flow $\mathbf{u}(\mathbf{x}, t)$ and of the perturbation to this flow due to the other particles. Formally, this perturbation $\mathbf{u}^{(i)}$ on the *isolated* i th particle due to another particle j of radius a at a distance $|\mathbf{r}^{(j)}|$ and moving with a velocity $\mathbf{v}^{(j)}$ can be written as a combination of a Stokeslet and a potential dipole flow as follows (see Wang *et al.* 2009):

$$\mathbf{u}^{(i)} = \left[\frac{3}{4} \frac{a}{|\mathbf{r}^{(j)}|} - \frac{3}{4} \frac{a^3}{|\mathbf{r}^{(j)}|^3} \right] \frac{\mathbf{r}^{(j)}}{|\mathbf{r}^{(j)}|^2} (\mathbf{v}^{(j)} \cdot \mathbf{r}^{(j)}) + \left[\frac{3}{4} \frac{a}{|\mathbf{r}^{(j)}|} + \frac{1}{4} \frac{a^3}{|\mathbf{r}^{(j)}|^3} \right] \mathbf{v}^{(j)}. \quad (4.1)$$

In a system of N particles, the net perturbation on the flow field experienced by any particle i is obtained by summing over the contributions made by each of the other $(N - 1)$ particles. Given the structure of the equations, for a system of N particles, it is impossible to solve exactly the perturbation field. Thus various approximations and iterative schemes become essential. However, in the present problem being studied in this paper, which involves two particles only, it is possible to solve exactly the hydrodynamic interaction term as it involves merely an inversion of a 6×6 matrix.

Let us now try to understand the effect of hydrodynamic interactions on the particle dynamics from a theoretical point of view. Without any loss of generality, and considering only two-particle interactions, let us consider a model where the two particles approach each other with the same velocity \mathbf{v} . A direct consequence of this model is that the perturbation $\mathbf{u}^{(1)}$ on particle 1 due to particle 2 is equal and opposite to the perturbation $\mathbf{u}^{(2)}$ on particle 2 due to particle 1, i.e. $\mathbf{u}^{(1)} = -\mathbf{u}^{(2)}$. The equation of motion for particle 1 can be written as

$$\frac{d\mathbf{v}}{dt} = -\frac{1}{\tau} (\mathbf{v} - \mathbf{u}_1 - \mathbf{u}^{(2)}); \quad (4.2)$$

$$\mathbf{u}^{(2)} = \left(\mathbf{v} + \frac{1}{2} \boldsymbol{\sigma} \mathbf{r} - \mathbf{u}^{(1)} \right) \left(\frac{3}{2} \frac{a}{|\mathbf{r}|} - \frac{1}{2} \frac{a^3}{|\mathbf{r}|^3} \right), \quad (4.3)$$

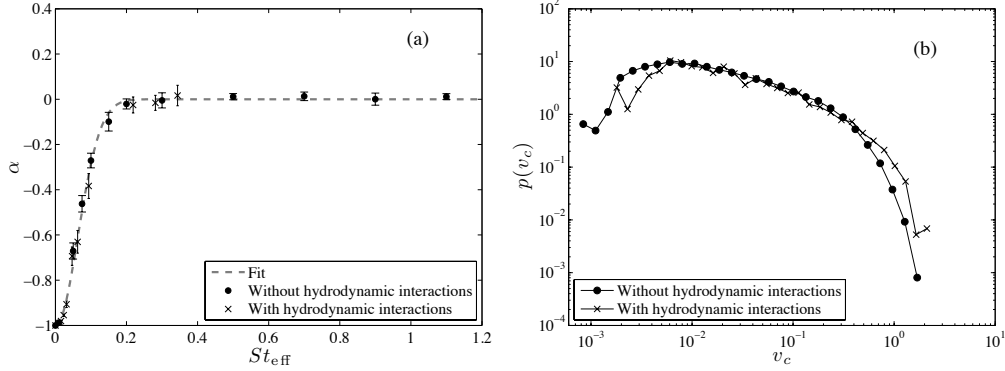


FIGURE 3. (a) Exponents α of the two-particle distribution $p_2(r) \propto (r - 2a)^\alpha$, along with their error bars. The case *with* hydrodynamic interactions (\times) is represented versus $St_{\text{eff}} = (5/16) St$ and that *without* interactions (\bullet), as a function of St ; the gray dashed line is the empirical fit $-\exp(-(St/0.09)^2)$ discussed in previous section. (b) PDF of inter-collision radial velocity v_c obtained from simulations with hydrodynamic interactions (\times) for $St = 0.15$, that is $St_{\text{eff}} = 0.047$ and without hydrodynamic interactions (\bullet) for $St = 0.05$.

where σ denotes the unperturbed fluid velocity gradient. Since, at the point of collision, $|\mathbf{r}| = 2a$, one has

$$\mathbf{u}^{(1)} = -\frac{11}{5} (\mathbf{v} - 2\sigma \hat{\mathbf{r}} a). \quad (4.4)$$

By using Eq. (4.4) in Eq. (4.3), we eventually obtain

$$\frac{d\mathbf{v}}{dt} = -\frac{16}{5\tau} (\mathbf{v} - 2\sigma \hat{\mathbf{r}} a). \quad (4.5)$$

The above analysis shows that the effect of long-range hydrodynamic interactions reduces in the vicinity of collisions to the dynamics in absence of interactions but with an effective Stokes number, which is equal to the actual Stokes number reduced by a factor of $16/5 = 3.2$. Thus a system of particles with a Stokes number St and subject to hydrodynamic interactions can be replaced by a system of particles, *without* any hydrodynamic interactions but with an effective Stokes number $St_{\text{eff}} = (5/16) St$ when we consider their statistical properties for very small inter-particle separations.

To confirm the arguments presented above we resort once more to numerical simulations by implementing the long-range hydrodynamic interactions (4.1). We use values of St between 0.05 and 1.1 as we had used for the case without any interaction terms. We begin by measuring the values of the exponent α introduced in the previous Section that describes the behaviour of the inter-particle distance distribution. Figure (3a) shows the values of α obtained as a function of the effective Stokes number $St_{\text{eff}} = (5/16) St$ (crosses); our data seems to fall, within error bars, on the empirical fit shown by a dashed gray line. To make the comparison more illuminating we plot on the same graph and as a function of the actual Stokes number St , the values of α (black dots) obtained from numerical simulations without hydrodynamic interactions, and already shown in Fig. (1b). Furthermore, in Fig. (3b) we show the PDF of the inter-collision velocity $p(v_c)$ as a function of v_c , on a log-log scale, for $St = 0.05$ obtained from a simulation *without* hydrodynamic interactions (black dots) and for $St = 0.15$ obtained from a simulation *with* hydrodynamic interactions (crosses). The two PDFs are nearly overlapping as our arguments before would suggest that the effective Stokes is $St_{\text{eff}} = 0.047 \approx 0.05$ for the case with the hydrodynamic interactions.

Our results suggest that hydrodynamic interactions increase the efficiency of dissipative mechanisms in terms of a reduction of the effective Stokes number. However, such considerations can only lead to qualitative deductions as our study account for long-range interactions only. The effect of lubrication forces will become dominant for particles at very small separations. On the one hand, this type of interaction is expected to decrease the collision efficiency between particles (see, e.g., Wang *et al.* 2005). On the other hand, lubrication is expected to increase damping when particles get close to each other; this effect is usually modelled by a restitution coefficient less than unity. Because of these two competing mechanisms, it is difficult to predict whether short-range hydrodynamic interactions will enhance or diminish the sticky elastic collision phenomenon.

5. Conclusions

In our work we have considered the effect of elastic collisions on the clustering of inertial particles. In particular we have investigated their influence on the probability distribution of inter-particle distance. Surprisingly, our findings differ markedly from the naive picture that collisions might only introduce a small-scale molecular chaos. We observe that the small-distance statistics is dominated by a phenomenon, which we call *sticky elastic collisions*, during which particles undergo a very large number of collisions during a time of the order of the fluid correlation time. It is interesting to note that these sticky elastic collisions remarkably resembles inelastic collapses observed in granular media, even though the underlying assumption in granular media (conservative inter-collision dynamics and dissipative collisions) is exactly the opposite of what we have considered here. In addition we have investigated the effect on this phenomenon of long-range hydrodynamic interactions between particles. Our results seem to indicate that the most significant effect at small scales of such interactions is to introduce an effective Stokes number. The problem of investigating the effect on sticky elastic collisions of short-range hydrodynamical interactions requires more rigorous theoretical understanding and more elaborate numerical simulations.

In this study we have focused on two-particle interactions. It is clear that the phenomena of sticky elastic collisions will be present even for large numbers of interacting particles. In this light, collective phenomena may emerge and provide a new mechanism to dissipate kinetic energy in violent collisions between particles. There are still many open questions concerning the stability of coalescence processes for the high impact velocities that are observed in turbulent settings. In particular, estimates on relative velocities between meter-sized objects in circum-stellar disks are by far too large to allow for their accretion and growth to form planet embryos (Wurm *et al.* 2001). The dissipative mechanisms relating to sticky elastic collisions might play a role there.

We would like to thank G. Falkovich and D. Mitra for useful discussions and acknowledge support from the European Cooperation in Science and Technology (EU COST) Action MP0806. The research leading to these results has received funding from the European Research Council under the European Community's Seventh Framework Program (FP7/2007-2013, Grant Agreement no. 240579) and from the Agence Nationale de la Recherche (Programme Blanc ANR-12-BS09-011-04).

REFERENCES

- BEC, J., BIFERALE, L., BOFFETTA, G., CENCINI, M., LANOTTE, A.S., MUSACCHIO, S. & TOSCHI, F. 2007 Heavy particle concentration in turbulence at dissipative and inertial scales. *Phys. Rev. Lett.* **98**, 084502.

- BEC, J., BIFERALE, L., CENCINI, M., LANOTTE, A.S. & TOSCHI, F. 2010 Intermittency in the velocity distribution of heavy particles in turbulence. *J. Fluid Mech.* **646**, 527–536.
- CALZAVARINI, E., KERSCHER, M., LOHSE, D. & TOSCHI, F. 2008 Dimensionality and morphology of particle and bubble clusters in turbulent flow. *J. Fluid Mech.* **607**, 13–24.
- CSANADY, G. 1980 *Turbulent diffusion in the environment*. Geophysics and Astrophysics Monographs Vol. 3 D. Reidel Publishing Company.
- DOUADY, S., COUDER, Y. & BRACHET, M.-E. 1991 Direct observation of the intermittency of intense vorticity filaments in turbulence. *Phys. Rev. Lett.* **67**, 983–986.
- FALKOVICH, G., FOUXON, A. & STEPANOV, M. 2002 Acceleration of rain initiation by cloud turbulence. *Nature* **419**, 151–154.
- FALKOVICH, G. & PUMIR, A. 2007 Sling effect in collision of water droplet in turbulent clouds. *J. Atm. Sci.* **64**, 4497–4505.
- GOLDHIRSCH, I. 2003 Rapid granular flows. *Ann. Rev. Fluid Mech.* **35**, 267–293.
- JEFFREY, D. J. & ONISHI, Y. 1984 Calculation of the resistance and mobility functions for two unequal rigid spheres in low-Reynolds-number flow. *J. Fluid Mech.* **139**, 261–290.
- POST, S. & ABRAHAM, J. 2002 Modeling the outcome of drop-drop collisions in Diesel sprays. *Intl. J. Multiphase Flow* **28**, 997–1019.
- TEN CATE, A., DERKSEN, J.J., PORTELA, L.M. & VAN DEN AKKER, H.E.A. 2004 Fully resolved simulations of colliding monodisperse spheres in forced isotropic turbulence, *J. Fluid Mech.*—/ **519**, 233–271.
- SAFFMAN, P.G. & TURNER, J.S. 1956 On the collision of drops in turbulent clouds. *J. Fluid Mech.* **1**, 16–30.
- SALAZAR, J.P.L.C. AND COLLINS, L.R. 2012 Inertial particle relative velocity statistics in homogeneous isotropic turbulence. *J. Fluid Mech.* **696**, 45–??.
- SHAW, R.A. 2003 Particle-turbulence interactions in atmospheric clouds. *Ann. Rev. Fluid Mech.* **35**, 183–227.
- SQUIRES, K.D. & EATON, J.K. 1991 Preferential concentration of particles by turbulence. *Phys. Fluids A* **3**, 1169–1178.
- SUNDARAM, S. & COLLINS, L.R. 1997 Collision statistics in an isotropic particle-laden turbulent suspension. Part 1. Direct numerical simulations. *J. Fluid Mech.* **335**, 75–109.
- WANG, L.P., AYALA, O., KASPRZAK, S.E. & GRABOWSKI, W.W. 2005 Theoretical formulation of collision rate and collision efficiency of hydrodynamically interacting cloud droplets in turbulent atmosphere, *J. Atmos. Sci.* **62**, 2433–2450.
- WANG, L.-P., ROSA, B., GAO, H., HE, G & JIN, G 2009 Turbulent collision of inertial particles: Point-particle based, hybrid simulations and beyond. *Intl. J. of Multiphase Flow* **35**, 854–867.
- WILKINSON, M. & MEHLIG, B. 2005 Caustics in turbulent aerosols, *Europhys. Lett.* **71**, 186–192.
- WURM, G., BLUM, J. & COLWELL, J.E., A new mechanism relevant to the formation of planetesimals in the solar nebula, *Icarus* **151**, 318–321.